Journal of Structural Chemistry. Vol. 59, No. 4, pp. 877-883, 2018.

GRAPHENE AND GRAPHITE SUPPORTS FOR SILICENE STABILIZATION: A COMPUTATION STUDY

A. E. Galashev, O. R. Rakhmanova, and K. A. Ivanichkina

The methods of molecular dynamics were used to study structural changes observed in bilayer silicene and thin slices of an ordinary Si crystal when transferred to the graphite substrate. The shape of the radial distribution function indicates noticeable distortion of the long-range order in the Si crystalline film. The first high peak of this function indicates honeycomb lattice in silicene. The motion the lithium ion in the silicene-graphene channel has been studied. The external strengthening of the silicene channel with graphene sheets not only increases its firmness but also improves the passage of intercalated lithium ions through this channel. The stresses in the channel walls are substantially decreased due to vacancy defects. Defects in the form of hexa-vacancies preserve their shape better than others defects when lithium ions pass through the channel.

DOI: 10.1134/S0022476618040194

Keywords: lithium, molecular dynamics, self-diffusion, silicene, structure.

INTRODUCTION

Silicene, a honeycomb lattice of silicon atoms, attracts considerable interest both in terms of fundamental research and applications to electronics. According to theoretical calculations, silicene should exhibit physical properties similar to those of graphene, in particular, massless Dirac fermions, quantum spin Hall effect, and possibly superconductivity [1]. The bonds between silicon atoms in silicene are formed due to mixed sp^2/sp^3-hybridization [2]. Strong interaction between silicene and the substrate can significantly depreciate remarkable electronic properties of this two-dimensional (2D) material [3], like it was observed in the epitaxial silicene layer on the Ag(111) surface [4]. A recent study reported a silicon monolayer, covering up to 80% of the substrate area, to be grown on highly oriented pyrolytic graphite at room temperature [5]. Along with silicene, small (up to 1 nm high) silicon clusters were formed on the surface. Band structure calculations of silicene on graphite substrates demonstrated the presence of Dirac cones.

One exceptional property of silicon is to trap an extraordinary number of lithium atoms as a result of intercalation (4.4 Li atoms per one Si atom) [6]. Therefore, silicene is one of the best candidates to be used as anode material in next generation lithium-ion batteries (LIB) [7]. It was discovered that Si nanoparticles or thin Si films, in contrast to 3D crystalline silicon, can help to some extent avoid the problem of silicon anodes destruction during lithiation/delithiation cycles [8]. In this respect, bilayer silicene appears especially promising, since it can be obtained easier than monolayer silicene [9]. The success of using silicene as a LIB anode material depends largely on the substrate used during intercalation/deintercalation cycles.

Institute of High-Temperature Electrochemistry, Ural Branch, Russian Academy of Sciences, Yekaterinburg, Russia; galashev@ihte.uran.ru. Translated from *Zhurnal Strukturnoi Khimii*, Vol. 59, No. 4, pp. 914-920, May-June, 2018. Original article submitted August 14, 2017.

This work aims at studying the stability of thin silicon films on graphite and the effectiveness of using graphene supports for bilayer silicene, including polyvacancy silicene, when used as the anode of lithium-ion batteries.

COMPUTATION MODEL

The calculations were carried out using the method of molecular dynamics (MD). The interactions in silicene were modeled by the Tersoff potential using the parameters from work [10]. The interaction between Si atoms from different silicene sheets was described by the Morse potential [11]. The same potential was used to describe the interaction between the lithium ion and Si atoms [9, 12, 13]. The numerical solution of equations of motion was obtained using the Runge-Kutta fourth-order method with a time step $\Delta t = 1\times10^{-16}$ s.

We consider here a reconstruction of a 4×4 surface. The unit cell of this silicene structure contains 18 Si atoms. Six of them are shifted by 0.064 nm along the normal to the surface, while the rest of them remain on the same (initial) plane. Such structure of silicene sheets is close to the silicene surface observed on the Ag(111) substrate [14]. If Si atoms appear above the initial surface in the upper sheet of bilayer silicene, then the atoms of the lower sheet will be shifted downwards.

Graphite formed by 3775 carbon atoms was represented by five graphene layers (755 atoms in each layer) arranged according to the scheme *AB AB*… with the interlayer distance $h = 0.371$ nm. The interatomic distance within the layers was 0.142 nm. The layers of the system were parallel to the plane $x0y$. Here we will study two types of Si films on graphite. The first type is a film made up of ten Si(100) layers with a diamond-like silicon lattice and interatomic distance $r_{\text{Si–Si}} = 0.234$ nm, and the second type is bilayer silicene with the interplanar distance 0.2481 nm obtained from density functional theory calculations [15]. Both these silicene sheets possess the reconstructed 4×4 surface. The Si(001) film contained 1280 atoms, while bilayer silicene was formed by 600 Si atoms. The distance between silicene sheets and graphene (graphite sheet) was the same as in [15], i.e. 0.222 nm. Free boundary conditions were applied to the entire system in three directions of coordinate axes. The simulation was performed at a temperature of 300 K in the *NVT*-ensemble. The first stage concerned modeling the films and the substrate separated from each other in a vacuum. The duration of these calculations was 50 ps, which was enough for each system to come into equilibrium by establishing the Maxwell distribution of atomic velocities. Then, the film and the substrate were brought into contact, and the main calculation was carried out with the duration of 200 ps.

The effectiveness of graphene supports for silicene channels was studied by simulating a lithium ion moving along the channel in an electric field. This motion was studied for the gap $h_g = 0.75$ nm between the silicene sheets. The fixation of the edges of silicene sheets preserves the gap h_g constant along the perimeter of the channel to avoid rotation of the sheets due to resultant torque occurring as a result of the Tersoff potential applied to two-dimensional systems [16, 17].

Perfect silicene sheets of 300 atoms each had rectangular dimensions of 4.7×4.0 nm (12 atoms along each edge of the sheet). Nine mono- or polyvacancies were distributed approximately uniformly over the area of the silicene sheet, so that the number of Si atoms in each sheet was 291, 282, 273, and 246 for the sheets with mono-, bi-, tri-, and hexa-vacancies, respectively. A constant electric field of 10^5 V/m sufficient to make the Li^+ ion pass the entire channel was directed along the axis $0x$ oriented in the "zigzag" direction of graphene sheets. Graphene sheets were placed parallel to the silicene sheets outside the channel. The front edges of graphene and silicene sheets were aligned with each other. The rectangular graphene sheet contained 820 atoms (20 atoms along each edge). The initial position of the ion corresponded to the channel height $h_g/2$. The ion was located near the middle of the sheet along the coordinate y and slightly shifted ($x = 0.198$ nm) inside the silicene channel.

As a rule, the duration of each calculation with the gap h_g was 1.5 million time steps, but in some cases the calculation was extended to $2.0\times10^6\ \Delta t$.

The self-diffusion coefficient was calculated using the mean squared atomic displacement $\langle[\Delta\mathbf{r}(t)]^2\rangle$

$$D = \lim_{t\to\infty}\frac{1}{2\Gamma t}\langle[\Delta\mathbf{r}(t)]^2\rangle,$$

where Γ = 3 is the dimension of the space, ⟨…⟩ means averaging over time.

The surface roughness of silicene (the arithmetic mean deviation of the profile) was calculated as [18]

$$R_a = \frac{1}{N}\sum_{i=1}^{N} | z_i - \overline{z} |,$$

where N is the number of nodes (atoms) on the surface of silicene; z_i is the displacement of atom i in the direction of the axis $0z$; $\overline{z}$ is the mean coordinate z for silicene; the values of z_i and $\overline{z}$ refer to the same point of time.

The stresses $\sigma_u^z(l)$ across surface elements in 2D materials were calculated according to the procedure reported in [19], where l is the number of the surface element, the normals to the elements are parallel to the axis z; u indicates the direction of the force. The total stresses in the plane of the sheet were determined as [20]

$$\sigma_{zu} = \sum_{l=1}^{N_l} \sigma_u^z(l),$$

where N_l is the number of surface elements in a two-dimensional material divided in the selected direction.

The calculations were performed with the LAMMPS code [21] for parallel MD simulations, which we modified by adding the components for calculating kinetic and mechanical properties of the system. The calculations were performed on a hybrid computational cluster "URAN" of IMM UB RAS with the peak capacity of 216 Tflop/s and 1864 CPU.

RESULTS AND DISCUSSION

Fig. 1 shows configurations of the films on graphite substrates obtained as a result of the main MD calculation (200 ps). As can be seen, each subsystem preserves its integrity both in the case of Si(001) film on graphene and in the case of bilayer silicene. All surfaces of the Si(001) film, including lateral surfaces, are subject to considerable structural relaxation. In general, the upper surface of the film remains horizontal. Three graphite sheets closest to the film are substantially deformed. Both films have strong contact with the top graphite sheet. The lower silicene sheet undergoes strong structural changes, while the upper sheet (with the exception of individual edges) preserves the honeycomb structure and the horizontal surface. Only two upper graphites layer adjacent to silicene undergo substantial changes in their shape. The average distance between the silicon and graphite surfaces is preserved in both cases. The final value of cross-coupling energy $E_{\text{Si–C}}$ for the system with silicene (–1.45 eV/atom) is lower than for the system with the Si(001) film (–1.07 eV).

In general, the two-dimensional crystalline structure, though not completely perfect, is preserved in silicene on graphite. The radial distribution function (RDF) for the Si atom closest to the center of the sheet adjacent to graphite in both cases demonstrates numerous peaks corresponding to the regular structure (Fig. 2). When constructing this function, we considered the coordinates of Si atoms in the lower silicene sheet or in two lower (already mixed) crystalline layers of the Si(001) film. Remember that one crystalline layer of the silicon film contains 128 atoms. Therefore, the combined film layer

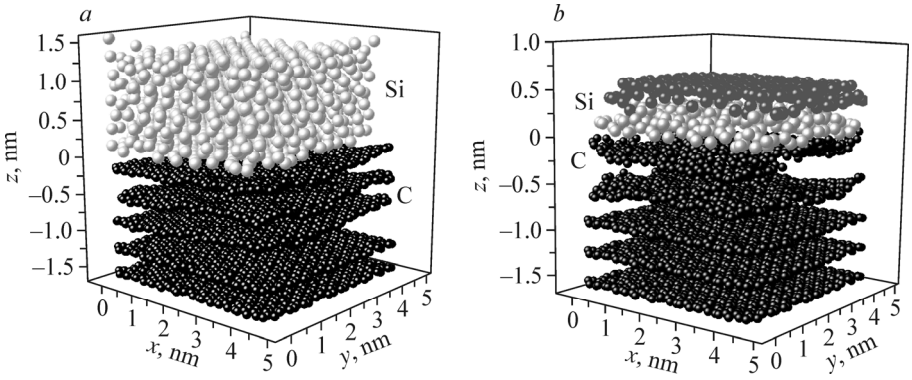

Fig. 1. System configuration: Si(001) film on graphite (*a*) and bilayer silicene on graphite (*b*) for the time instance of 200 ps.

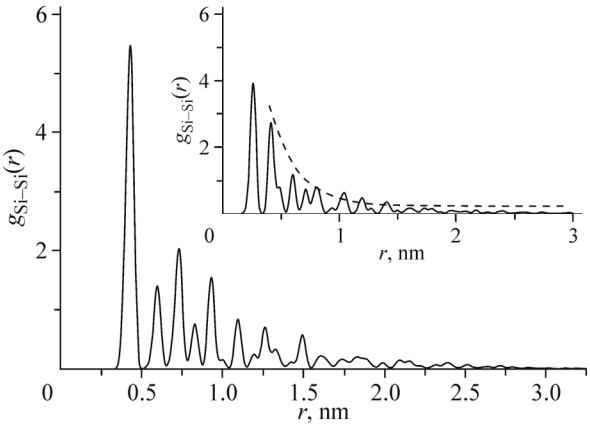

Fig. 2. Radial distribution function for the central atom of the lower (256 atomic) Si(001) film on graphite. The inset shows RDF for the lower silicene sheet on graphite.

contains 256 of Si atoms, which is closer to the number of atoms (N = 300) in the silicene sheet. The positions of the first two maxima of $g(r)$ in the combined lower film layer are close to those in the lower silicene sheet: r_{m1} = 0.24 nm, r_{m2} = 0.39 nm (in the film) and r_{m1} = 0.23 nm, r_{m2} = 0.40 nm (in silicene). The third peak (at 0.46 nm) exhibited by $g(r)$ for the lower layer of the Si(001) film is absent in the RDF of the lower silicene sheet. The following maxima appear at 0.57 nm for the Si(001) film and at 0.59 nm for silicene. An important characteristic feature of RDF for silicene is higher intensity of the first peak $g(r)$ relative to other peaks. As a consequence, the intensity ratios of the first four $g(r)$ peaks for the lower silicene sheet (1:0.46:0.30:0.23) are very different from those of the corresponding Si(100) film layer (1:0.75:0.54:0.37). In other words, short-range order or preservation of the honeycomb structure in silicene is the characteristic feature of silicene structure.

Fig. 3 shows the trajectory of a lithium ion in a constant electric field E inside the silicene-graphene channel, when each silicene sheet contains 9 monovacancies. After the starting point (*1*), the ion makes several vertical oscillations in the course of translational motion, approaches the exit and, after a short delay accompanied by rapidly increased vibrations, leaves the channel (point (2)). Both graphene sheets are buckled outwards.

The time taken by the ion to pass the defectless silicene-graphene channel was 42.2 ps, and this value was 3.4, 3.0, and 2.3 times smaller for the channels with mono-, tri-, and hexa-vacancies, respectively. Smaller times spent by the ion in the channels with defective walls can be explained by smaller number of collisions between the ion and Si atoms whose number decreases due to larger size of vacancies. The Li^+ ion stays for 200 ps inside the channel with bi-vacancies in the silicon walls. This can be explained by the fact that the size of relaxing bi-vacancies is most favorable for trapping lithium ions. The bonding energy between the ions and vacancy defects can substantially exceed the one between the ion and the corresponding Si atom [22].

Despite the presence of graphene support, the motion of the ion along the channel increased the roughness R_a of both sheets of perfect silicene and silicene with mono- and bi-vacancies (Fig. 4) with respect to the roughness of perfect silicene sheets at the initial instant of time R_{a0}^{per}. However, R_a decreases and becomes even smaller than R_{a0}^{per} in the presence of larger vacancies in silicene. The roughness in the lower silicene sheet is much higher than R_a of the upper sheet only for the case of silicene sheets with bi-vacancies. There is not enough free space in the plane of silicene sheets formed by mono- and bi-vacancies to change the preferential displacement of atoms from the vertical to the horizontal direction. However, the presence of tri-vacancies in silicene sheets makes such transition possible, and it preserves also in the case of hexa-vacancies. The inset to Fig. 5 shows time dependencies of the $R_a^{\text{vac}} / R_{a0}^{\text{per}}$ ratio for the upper and the lower silicene sheets in the case of bi-vacancies. The greatest relative error in determining the ratio obtained for the upper sheet of silicene does not exceed 8%.

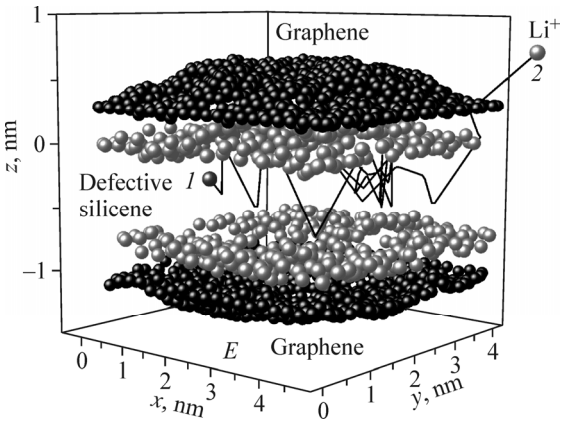

Fig. 3. Trajectory of the lithium ion inside the silicene channel supported from both sides by graphene sheets. The gap between the sheets is $h_g = 0.75$ nm, the motion occurs in a constant electric field E. Each silicene sheet contains 9 monovacancies; *1* and *2* are the initial and the final trajectory points, respectively.

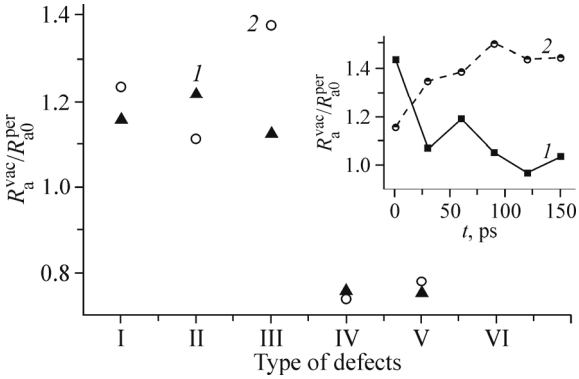

Fig. 4. Relative roughness of silicene sheets, depending on the type of their defects, obtained during the motion of the Li^+ ion inside the channel: *1* is the top sheet, *2* is the bottom sheet. The inset shows time dependences of relative roughness for the upper (*1*) and the lower (*2*) silicene sheets.

It is interesting to consider how the self-diffusion coefficient D_{Si} of Si atoms changes as a result of changing the relief of channel walls from defect-free to the one containing various types of vacancy defects. Fig. 5 shows the mobility characteristics of atoms D_{Si} of the lower and upper silicene sheets as well as the change of their mean values (dashed line). In general, the mobility of Si atoms increases nonmonotonically with the size of defects. However, the average atomic mobility even decreases in the case of monovacancies, and remains almost at the same level as in defect-free silicene in the case of tri-vacancies. It is noteworthy that there is a large difference between D_{Si} values of the lower and the upper silicene sheets with bi-vacancies, and very close values of this quantity for the corresponding sheets with hexa-vacancies. The large difference between D_{Si} can be explained by different effect of Li^+ ion on the mobility of atoms in the sheets with bi-vacancies, while close D_{Si} values for the sheets with hexa-vacancies are more likely due to sufficiently high stability of such structures.

Fig. 6 shows the absolute value of the total stress $|\sigma_{zy}|$ in silicene sheets as a function of the defects size. This characteristic of stress is the largest for almost all considered silicene sheets, with rare exceptions for the $|\sigma_{zx}|$ value. As can be seen, the magnitude of the stress in the lower silicene sheet (curve *2*) is always much larger than the corresponding

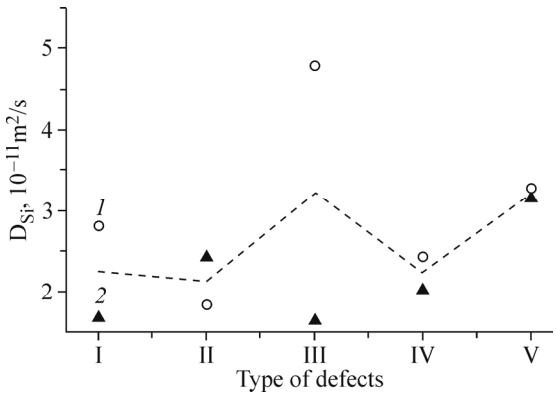

Fig. 5. Self-diffusion coefficient of Si atoms in the lower (*1*) and the upper (*2*) silicene sheet: I is the defectless silicene, II, III, IV, and V are silicenes with mono-, bi-, tri-, and hexa-vacancies, respectively. Dashed line shows the average mobility for two silicene sheets.

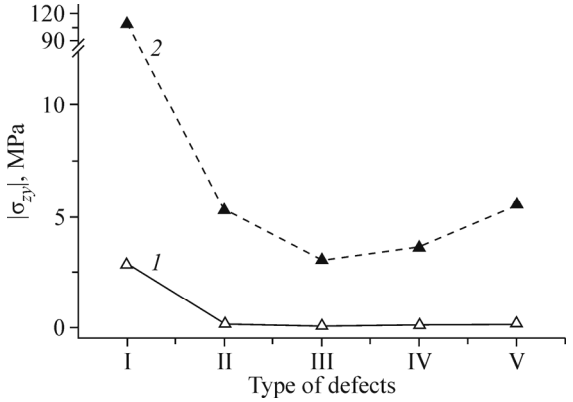

Fig. 6. Magnitude of total stress σ_{zy} in the lower (*1*) and the upper (*2*) sheet of perfect silicene (I) and silicene with mono- (II), bi- (III), tri- (IV), and hexa-vacancies (V).

characteristic of the upper sheet (curve *1*). Both the upper and the lower perfect silicene sheets possess much larger $|\sigma_{zy}|$ values than any corresponding sheet of defective silicene. The magnitude of stress σ_{zy} in the lower sheet decreases in silicene with mono- and bi-vacancies as compared to its value in defect-free silicene, and then the value increases for the cases of tri- and hexa-vacancies. Thus, starting with tri-vacancies, the dimensional effect of defects works in the opposite direction to increase the internal stress in silicene.

CONCLUSIONS

The calculations demonstrate the possibility of thin silicon films, including bilayer silicene, existing on graphite substrates. Silicene on graphite surface undergoes certain structural changes. A Si(001) film also undergoes structural relaxation when placed on graphite. Vertical displacement of Si atoms increases as a result of lattice misfit of silicene and graphene (graphite sheet) and substantial interaction between Si and C atoms. This, in turn, is accompanied by distortions in ideal horizontal projections of the silicene lattice and the diamond-like lattice.

A numerical characteristic was obtained for the stressed state developing in a silicene-graphene channel when a lithium ion passes through the channel. Vacancy defects in the silicene walls of the channel substantially reduce the stresses in silicene and graphene walls. Conductivity of the channel decreases in the case of bi-vacancies. Tri- and hexa-vacancies, in contrast to mono- and bi-vacancies, do not increase the roughness of silicene walls. Mono-, bi-, and tri-vacancies in silicene walls are subject to destruction when Li^+ ions move along the channel, which is explained by the fact that five-membered silicon rings are formed. Hexa-vacancies in silicene with graphene support demonstrate higher resistance to destruction.

Thus, the presence of polyvacancies in silicene causes some instability which hampers defective silicene to be used as anodes in lithium-ion batteries, but hexa-vacancies in silicene provide more stable functioning of the anode.

The study was supported by the Russian Science Foundation (grant No. 16-13-00061).

REFERENCES

1. L. Tao, E. Cinquanta, D. Chiappe, C. Grazianetti, M. Fanciulli, M. Dubey, A. Molle, and D. Akinwande. *Nat. Nanotechnol.*, **2015**, *10*, 227.
2. E. Cinquanta, E. Scalise, D. Chiappe, C. Grazianetti, B. van den Broek, M. Houssa, M. Fanciulli, and A. Molle. *J. Phys. Chem. C*, **2013**, *117*, 16719.
3. D. Tsoutsou, E. Xenogiannopoulou, E. Golias, P. Tsipas, and A. Dimoulas. *Appl. Phys. Lett.*, **2013**, *103*, 231604.
4. X. Xu, J. Zhuang, Y. Du, H. Feng, N. Zhang, C. Liu, T. Lei, J. Wang, M. Spencer, T. Morishita, X. Wang, and S. X. Dou. *Sci. Rep.*, **2014**, *4*, 7543.
5. M. De Crescenzi, I. Berbezier, M. Scarselli, P. Castrucci, M. Abbarchi, A. Ronda, F. Jardali, J. Park, and H. Vach. *ACS Nano*, **2016**, *10*, 11163.
6. A. E. Galashev, Yu. P. Zaikov, and R. G. Vladykin. *Rus. J. Electrochem.,* **2016**, *52*(10), 966.
7. A. E. Galashev, K. A. Ivanichkina, A. S. Vorob′ev, and O. R. Rakhmanova. *Phys. Solid State*, **2017**, *59*(6), 1242.
8. A. E. Galashev and K. A. Ivanichkina. *Rus. J. Phys. Chem. A*, **2017**, *91*(12), 2448.
9. O. R. Rakhmanova and A. E. Galashev. *Rus. J. Phys. Chem. A*, **2017**, *91*(5), 921.
10. J. Tersoff. *Phys. Rev. B*: *Condens. Matter.*, **1989**, *39*, 5566.
11. R. Yu, P. Zhai, G. Li, and L. Liu. *J. Electron. Mater.*, **2012**, *41*, 1465.
12. E. C. Angel, J. S. Reparaz, J. Gomis-Bresco, M. R. Wagner, J. Cuffe, B. Graczykowski, A. Shchepetov, H. Jiang, M. Prunnila, J. Ahopetto, F. Alzina, and C. M. Sotomayor Torres. *APL Mater.*, **2014**, *2*, 012113.
13. S. K. Das, D. Roy, and S. Sengupta. *J. Phys. F*: *Metal. Phys.*, **1977**, *7*, 5.
14. K. Kawahara, T. Shirasawa, R. Arafune, C.-L. Lin, T. Takahashi, M. Kawai, and N. Takegi. *Surf. Sci.*, **2014**, *623*, 25.
15. M. Neek-Amal, A. Sadeghi, G. R. Berdiyorov, and F. M. Peeters. *Appl. Phys. Lett.*, **2013**, *103*, 261904.

16. A. E. Galashev and Yu. P. Zaikov. *Rus. J. Phys. Chem. A,* **2015**, *89*, 2243.
17. A. E. Galashev and V. A. Polukhin. *Phys. Solid State,* **2013**, *55*, 1733.
18. A. E. Galashev and A. A. Galasheva. *High Energy Chem*., **2014**, *48*(2), 112.
19. A. E. Galashev. *Phys. Solid State*, **2014**, *56*, 1048.
20. A. E. Galashev and Yu. P. Zaikov. *Rus. J. Electrochem.,* **2015**, *51*, 867.
21. S. Plimpton. *J. Comp*. *Phys*., **1995**, *117*, 1.
22. A. Y. Galashev. *Mol. Simul.*, **2010**, *36*, 273.